Supplementary figure 1

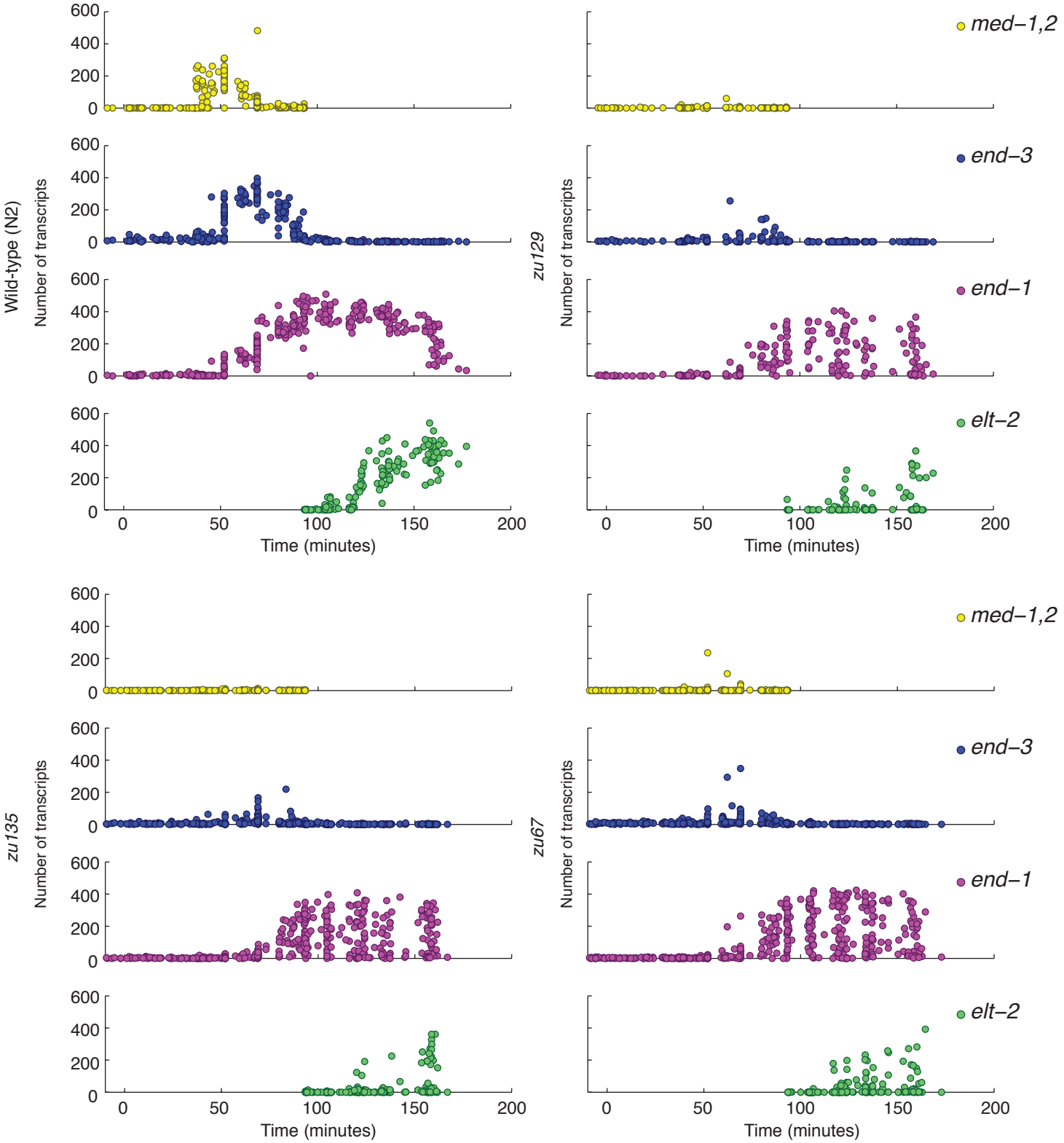

Supplementary Figure 1: Number of *med-1,2*, *end-3*, *end-1* and *elt-2* mRNAs in individual wild-type (N2) and *skn-1* (*zu129*, *zu135* and *zu67*) mutant embryos plotted as a function of developmental time (minutes from the first zygotic cell division). We computed developmental time from the number of nuclei by using the lineage data collected by Bao *et al.*, Developmental Biology, **318** (1):65-72, 2008: for a particular number of nuclei, those data allow one to assign a particular developmental time window during which the embryo contains that many nuclei, and we randomly assigned the time within that window. It is important to note that Bao *et al.* lineage data were collected at 20°C rather than 25°C (used in our study), so there is likely to be a conversion factor between the time indicated on our graphs and the actual time.

Supplementary figure 2

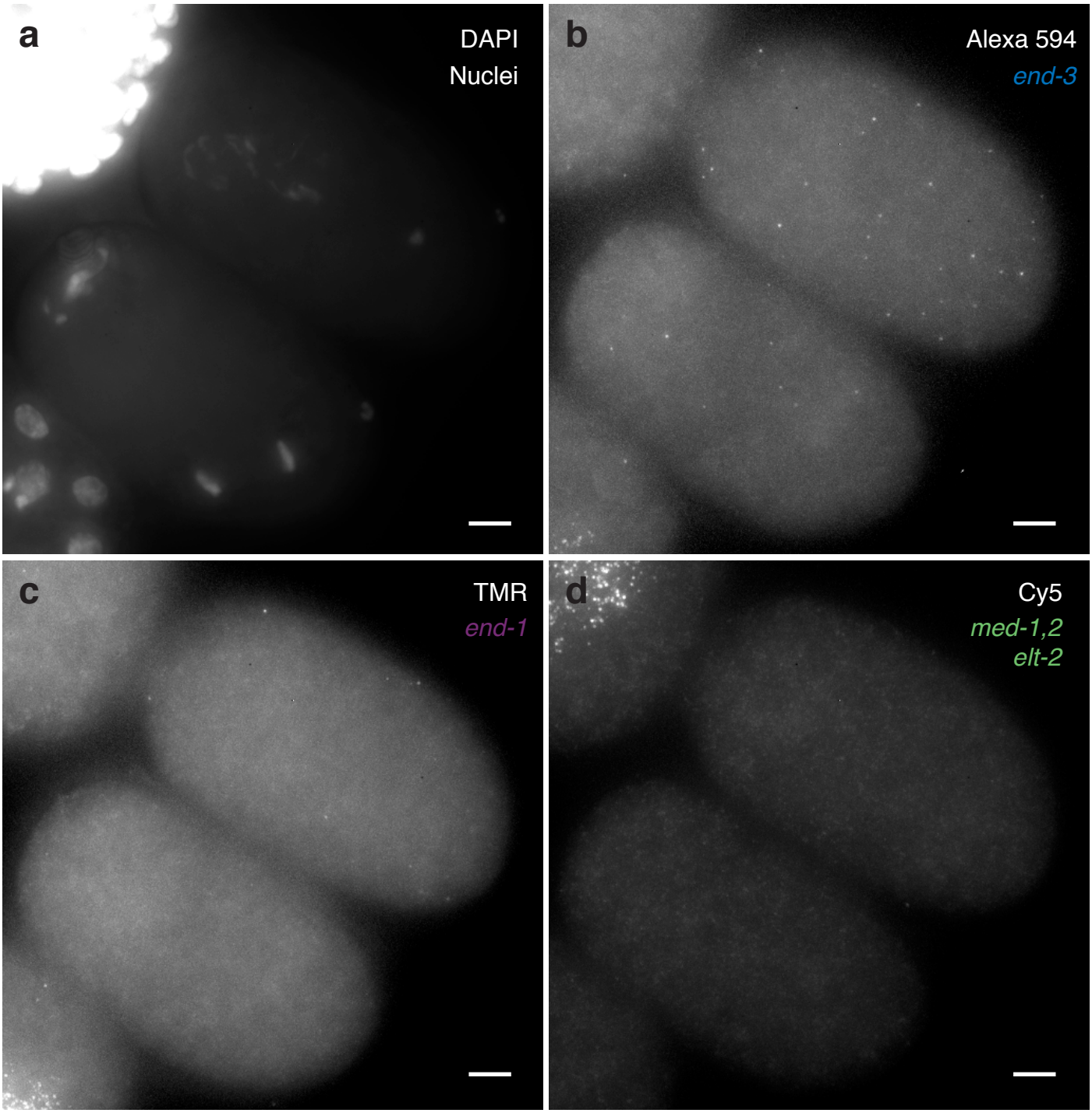

Supplementary Figure 2: *end-3* and *end-1* transcripts are maternally deposited while *med-1,2* are not. **a**. Image of the nuclei (stained with DAPI) of two *C. elegans* embryos, one at the early two-cell stage and one at the three-cell stage. **b-d**. Images of *end-3* (b), *end-1* (c) and *med-1,2/elt-2* (d) transcripts in the same two embryos. Images are maximum-projections of three dimensional microscope data. Scale bars are 5μm long.

Supplementary figure 3

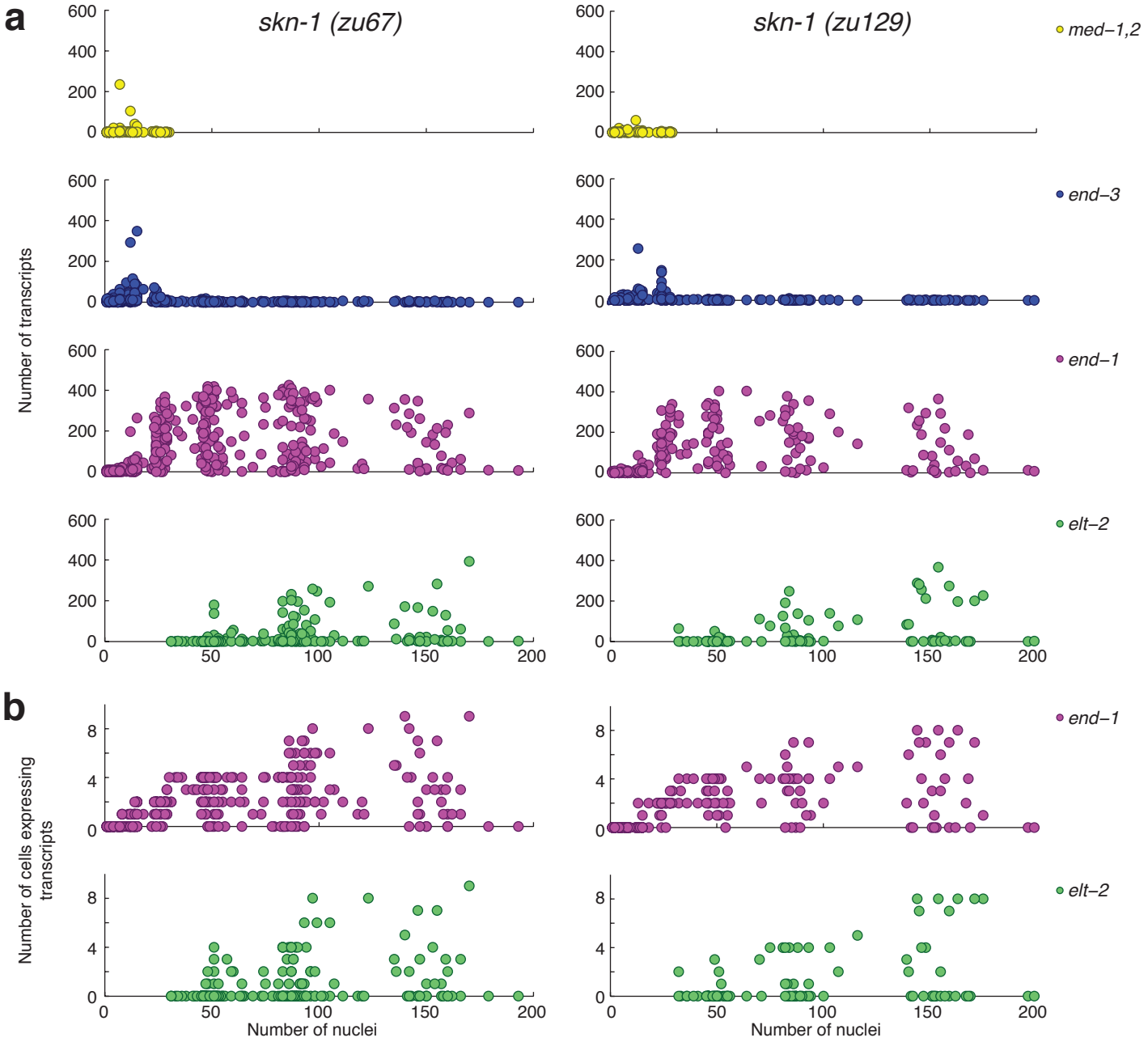

Supplementary Figure 3: **a**. Transcript number vs. number of nuclei for a collection of randomly staged *skn-1(zu67)* and *skn-1(zu129)* mutant early embryos. **b**. Number of cells expressing *end-1* (top) or *elt-2* (bottom) within individual *skn-1(zu67)* and *skn-1(zu129)* mutant embryos vs. number of nuclei.

Supplementary figure 4

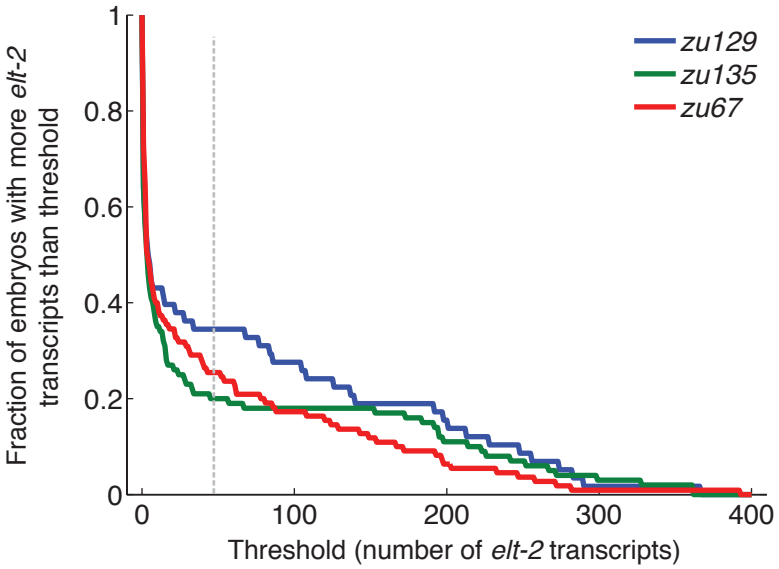

Supplementary Figure 4: Dependence of the penetrance of the *skn-1* mutant alleles (*zu129*, blue; *zu135*, green; *zu67*, red) upon the threshold in the level of *elt-2*. For each value of the *elt-2* threshold (x-axis), we calculated the fraction of embryos (between the 80 and 200 cell stages) with more *elt-2* transcripts than the threshold. The dotted line represents a threshold of 50 *elt-2* transcripts, which we used in our calculation of the threshold of the number of *end-1* transcripts required to activate *elt-2* (supplementary figure 8).

Supplementary figure 5

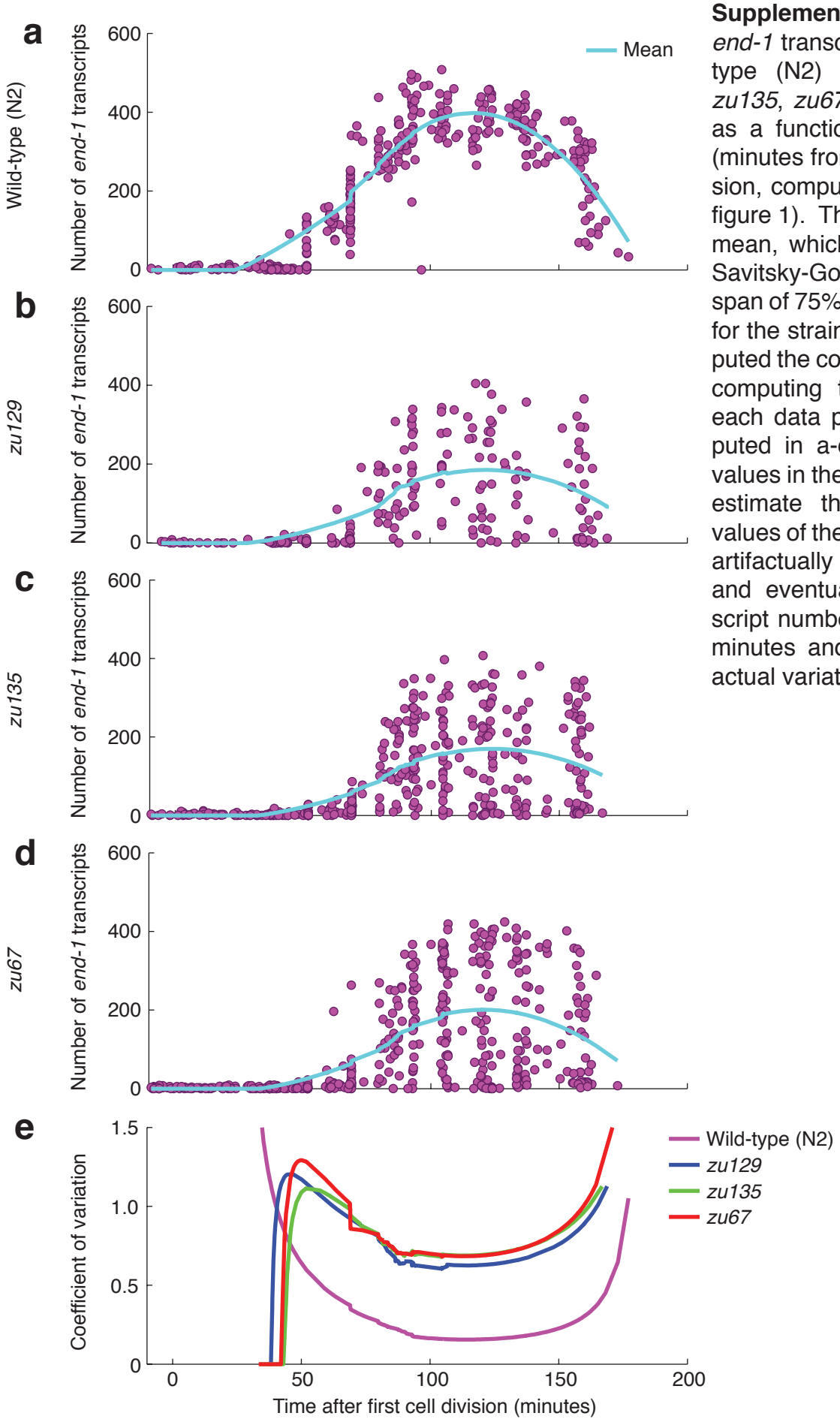

Supplementary Figure 5: Number of *end-1* transcripts in individual **a**. wild-type (N2) and **b-d**. *skn-1* (*zu129, zu135*, *zu67*) mutant embryos plotted as a function of developmental time (minutes from the first zygotic cell division, computed as per supplementary figure 1). The cyan line represents the mean, which we computed using the Savitsky-Golay method with a data span of 75%. **e**. Coefficient of variation for the strains shown in a-d. We computed the coefficient of variation by first computing the squared deviation of each data point from the mean computed in a-d., then smoothing those values in the same way as the mean to estimate the variance. While the values of the coefficient of variation are artifactually high during the initial rise and eventual decline of *end-1* transcript number, the values between 75 minutes and 150 minutes reflect the actual variation.

Supplementary figure 6

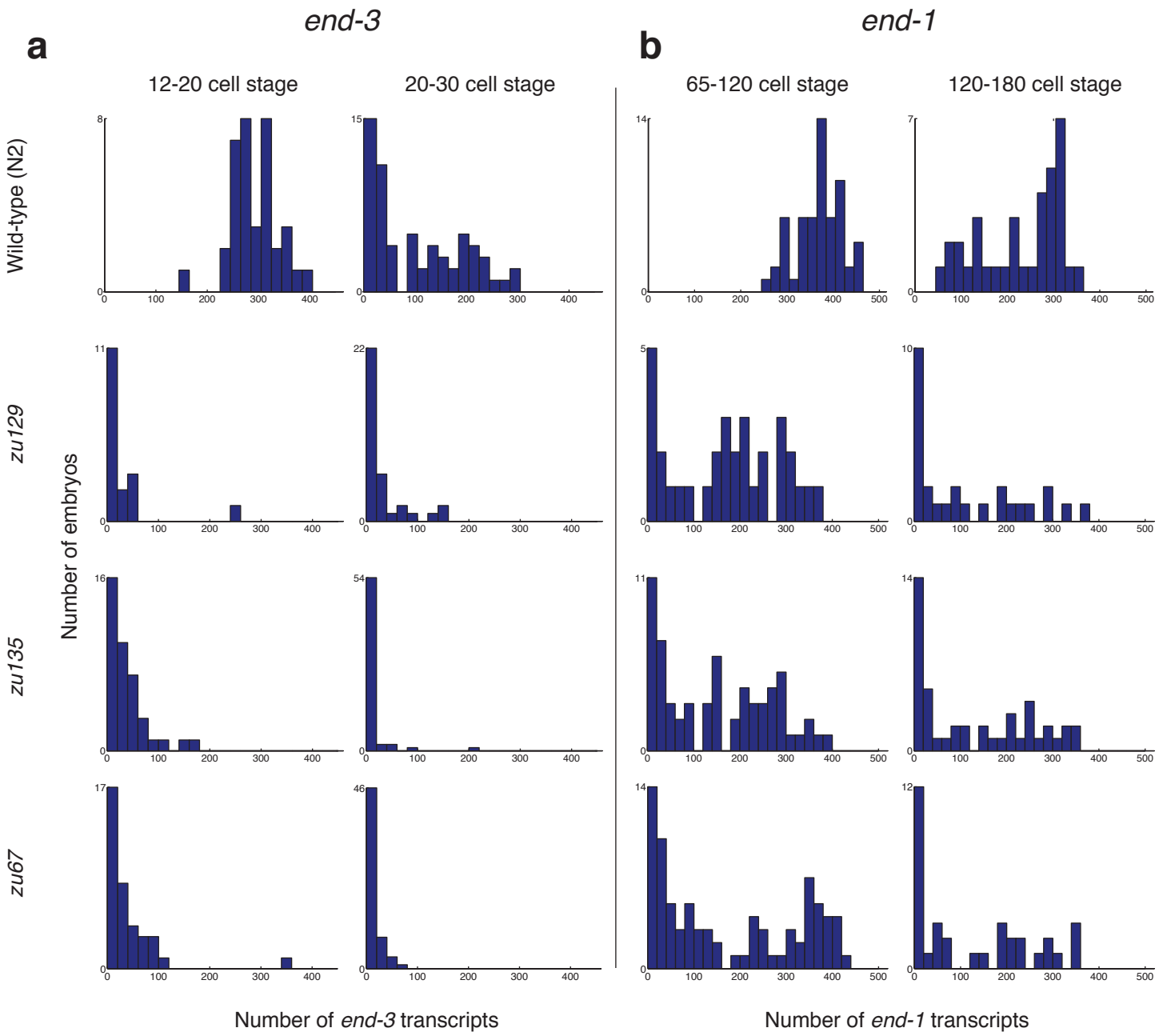

Supplementary Figure 6: Histograms of *end-3* and *end-1* transcript numbers in wild-type (N2) and *skn-1* mutant embryos (*zu67*, *zu135* and *zu129*). **a**. We generated *end-3* expression histograms for embryos containing between 12 and 20 nuclei (left) or 20 and 30 nuclei (right). **b**. We generated *end-1* expression histograms for embryos containing between 65 and 120 nuclei (left) or 120 and 180 nuclei (right). The purpose of examining the *end-3* expression distributions was to see if differences in *end-3* expression could explain the different penetrances of the various mutant alleles. Our data indicate that this is unlikely, since the levels of *end-3* expression are generally higher during the 10-20 cell stage in the more penetrant *zu67* and *zu135* alleles. The expression of *end-3* is somewhat higher in the less penetrant *zu129* allele during the 20-30 cell stage, but the cumulative level of END-3 protein is likely to be dominated by the differences in transcript number during the earlier time window.

Supplementary figure 7

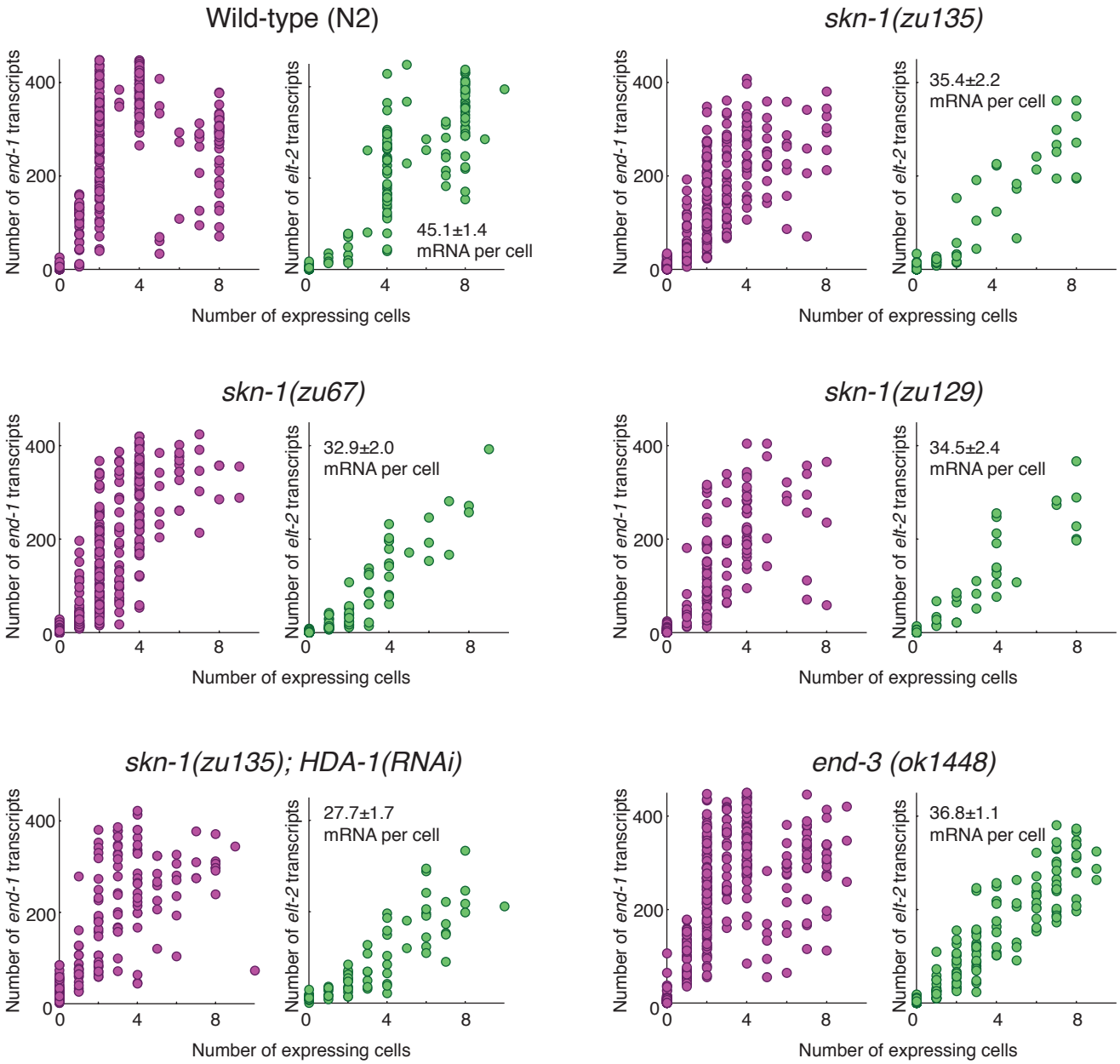

Supplementary Figure 7: Transcript number vs. number of expressing cells for both *end-1* and *elt-2* in all the strains used in this study. We computed the number of mRNA per cell using a least squares fit to compute the slope of the best fit line to the data; we computed the errors by bootstrapping.

Supplementary figure 8

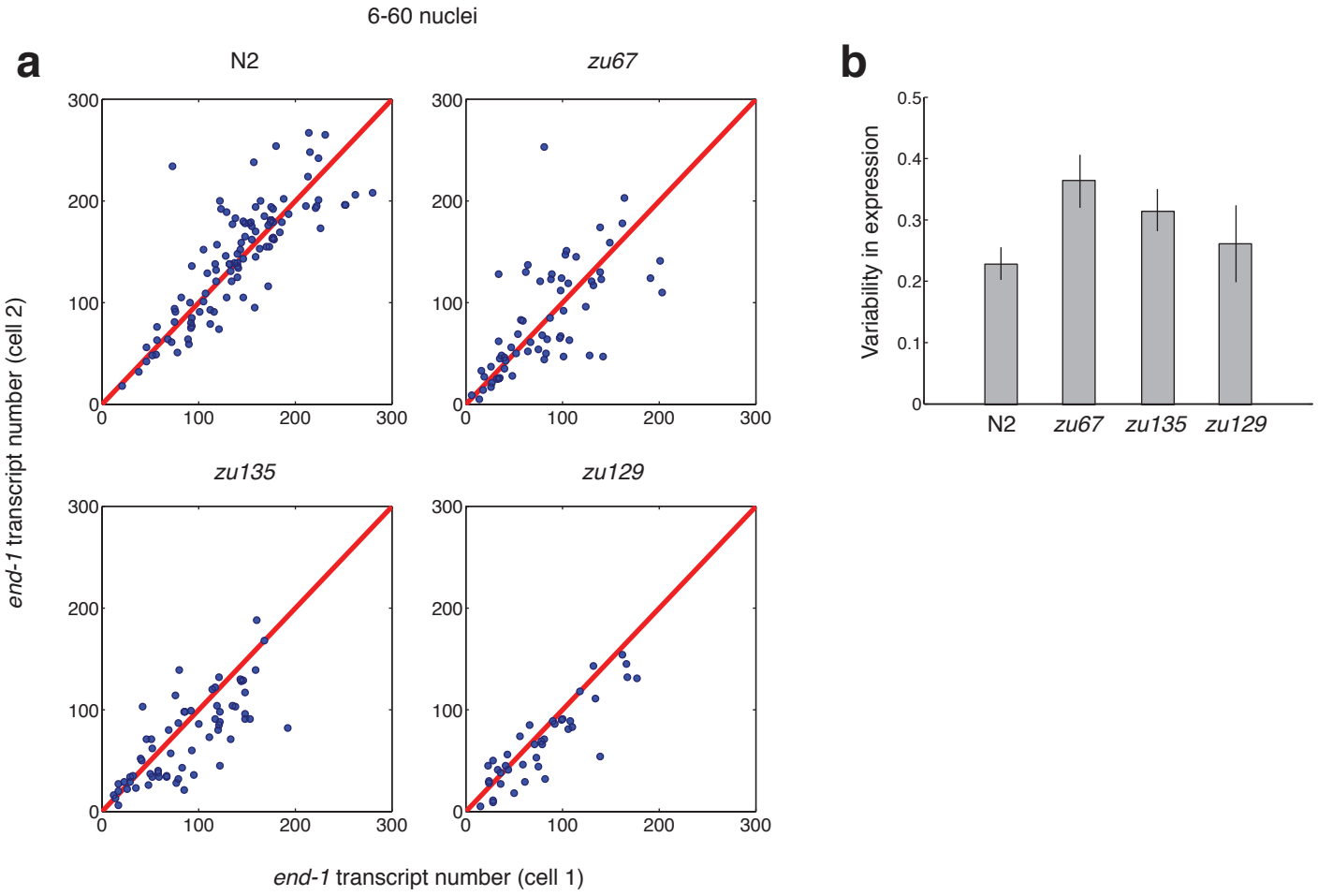

Supplementary Figure 8: **a**. We estimated the number of *end-1* transcripts in each cell in embryos (6-60 nuclei) in which two cells were expressing *end-1*, assigning mRNAs to the nearest nucleus. The x axis is the number of *end-1* nuclei in the one of the cells, and the y axis is the number of cells in the other cell (randomly chosen). The red line, y=x, represents equal expression in both cells; hence, deviation from this line represents variability. **b**. To quantify the variability, we computed (for each embryo) the difference in transcript number between the two cells divided by the mean transcript number in the two cells and calculated the root-mean-square deviation across all embryos in (a) (y axis). We computed the error bars by bootstrapping. In computing the variability, we excluded embryos in which either cell contained fewer than 50 *end-1* transcripts because there were few N2 embryos in that region. Despite potential errors in our cell-assignment method, we found significantly increased variability in both the *zu67* and *zu135* mutant alleles as compared to the wild type.

Supplementary figure 9

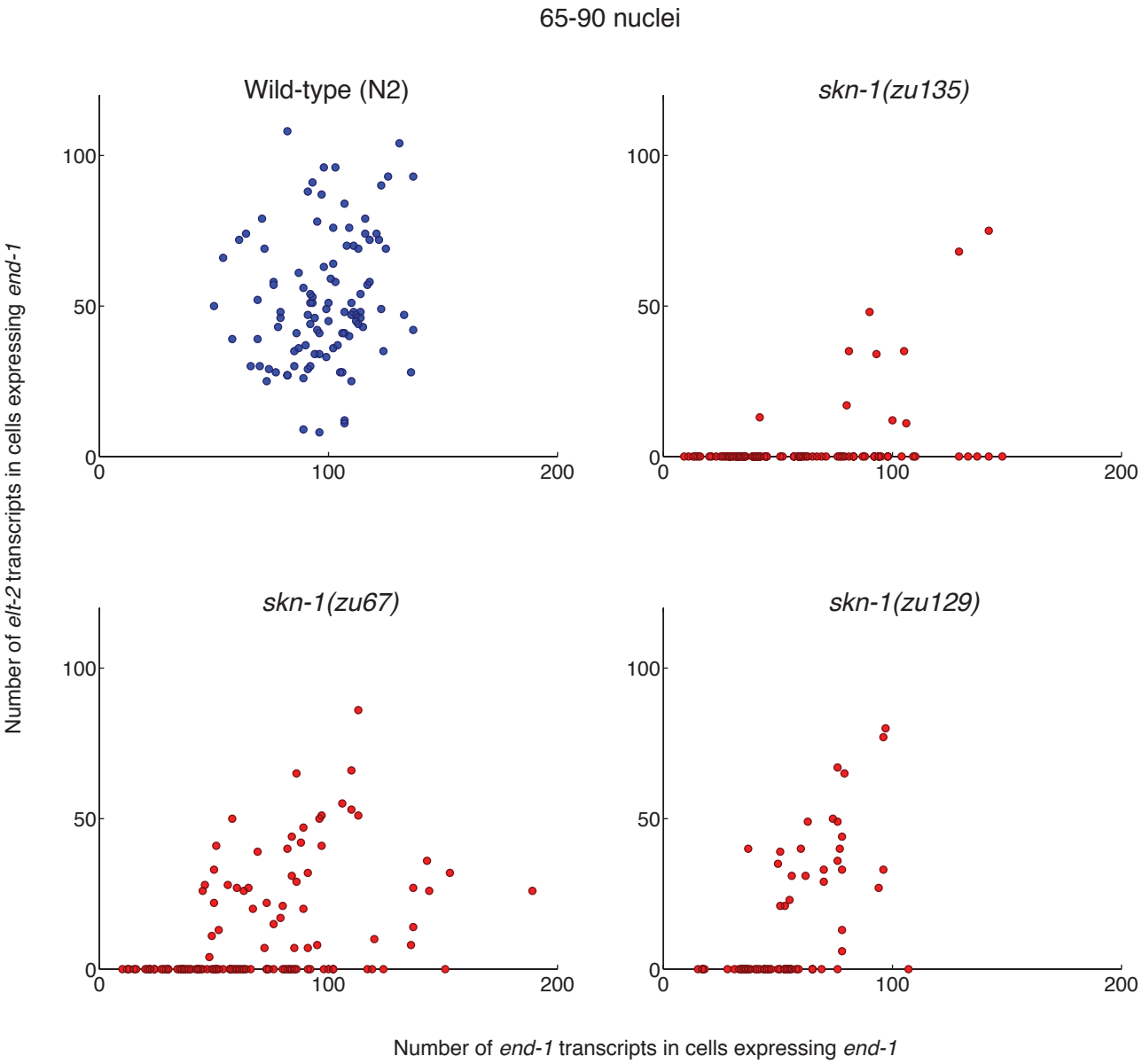

Supplementary Figure 9: Number of *elt-2* vs. *end-1* transcripts in individual cells expressing *end-1*. We used embryos containing between 65 and 90 nuclei in the wild type as well as the *skn-1* mutant alleles. We counted the number of mRNA in individual cells by assigning each mRNA to the closest nucleus (whose locations we identified manually).

Supplementary figure 10

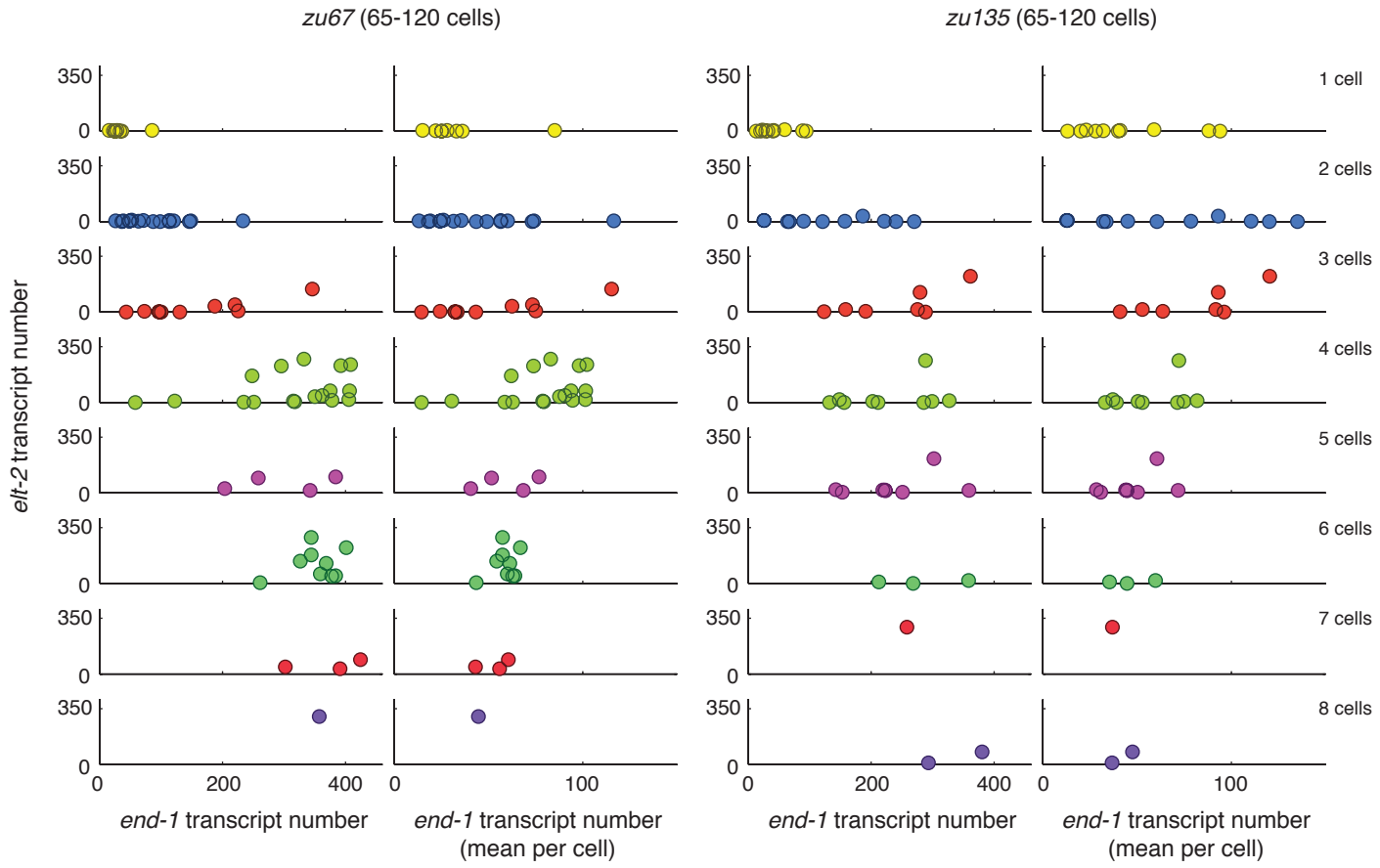

Supplementary Figure 10: Number of *elt-2* vs. *end-1* transcripts in *zu67*, *zu135* and *zu129* mutant embryos containing between 65 and 120 nuclei with 1 through 8 (top to bottom) cells expressing *end-1* (left); number of *elt-2* vs. average number of end-1 transcripts per cell in *zu67*, *zu135* and *zu129* mutant embryos containing between 65 and 120 nuclei with 1 through 8 (top to bottom) cells expressing *end-1* (right). The threshold of *end-1* required to activate *elt-2* (in the entire embryo) was perhaps somewhat independent of the number of cells expressing, although our data are somewhat sparse to make this conclusion.

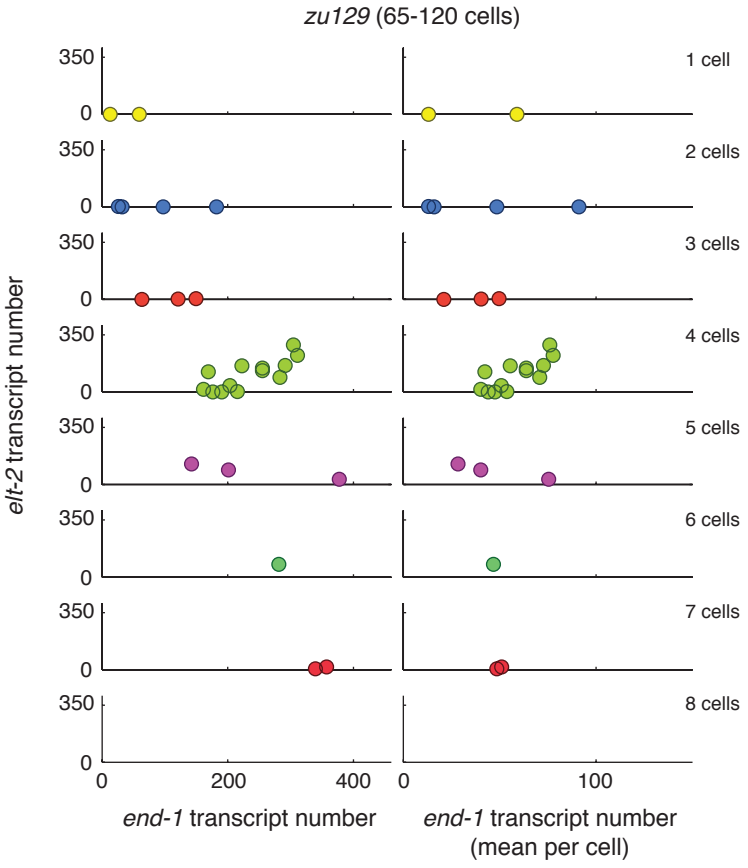

Supplementary figure 11

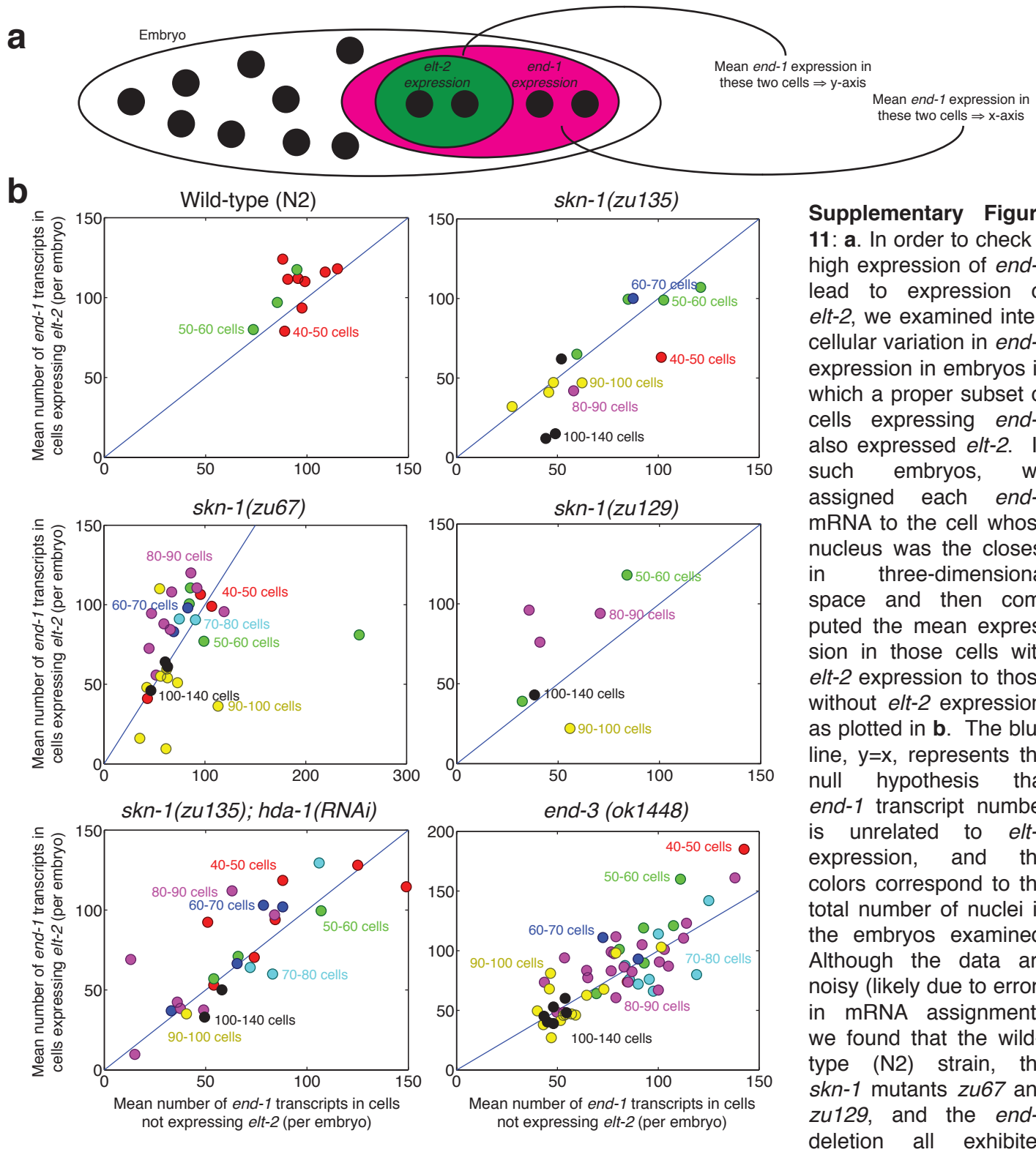

Supplementary Figure 11: **a**. In order to check if high expression of *end-1* lead to expression of *elt-2*, we examined inter-cellular variation in *end-1* expression in embryos in which a proper subset of cells expressing *end-1* also expressed *elt-2*. In such embryos, we assigned each *end-1* mRNA to the cell whose nucleus was the closest in three-dimensional space and then computed the mean expression in those cells with *elt-2* expression to those without *elt-2* expression, as plotted in **b**. The blue line, y=x, represents the null hypothesis that *end-1* transcript number is unrelated to *elt-2* expression, and the colors correspond to the total number of nuclei in the embryos examined. Although the data are noisy (likely due to errors in mRNA assignment), we found that the wild-type (N2) strain, the *skn-1* mutants *zu67* and *zu129*, and the *end-3* deletion all exhibited higher *end-1* expression in *elt-2* positive cells than in *elt-2* negative cells (i.e., above the blue line) at particular developmental stages (40-60 nuclei for N2; 60-90 for *skn-1* mutants, consistent with the developmental delay in *end-1* expression; 40-70 for *end-3* deletion). This shows that decision of whether or not to express *elt-2* is not made when there is just one E cell, with that early decision propagating to all subsequent E lineage cells. Moreover, in the *skn-1* mutants, whenever two of the three or four *end-1* positive cells expressed *elt-2*, those two cells were invariably next to each other, indicating that the decision to express *elt-2* was made one cell-cycle before and the decision was carried over through one division. This may imply that the decision window occurs when there are two E cells. The *skn-1(zu135); hda-1(RNAi)* data did not exhibit a discernible pattern, perhaps because of variability in the onset of the decision window.

Supplementary figure 12

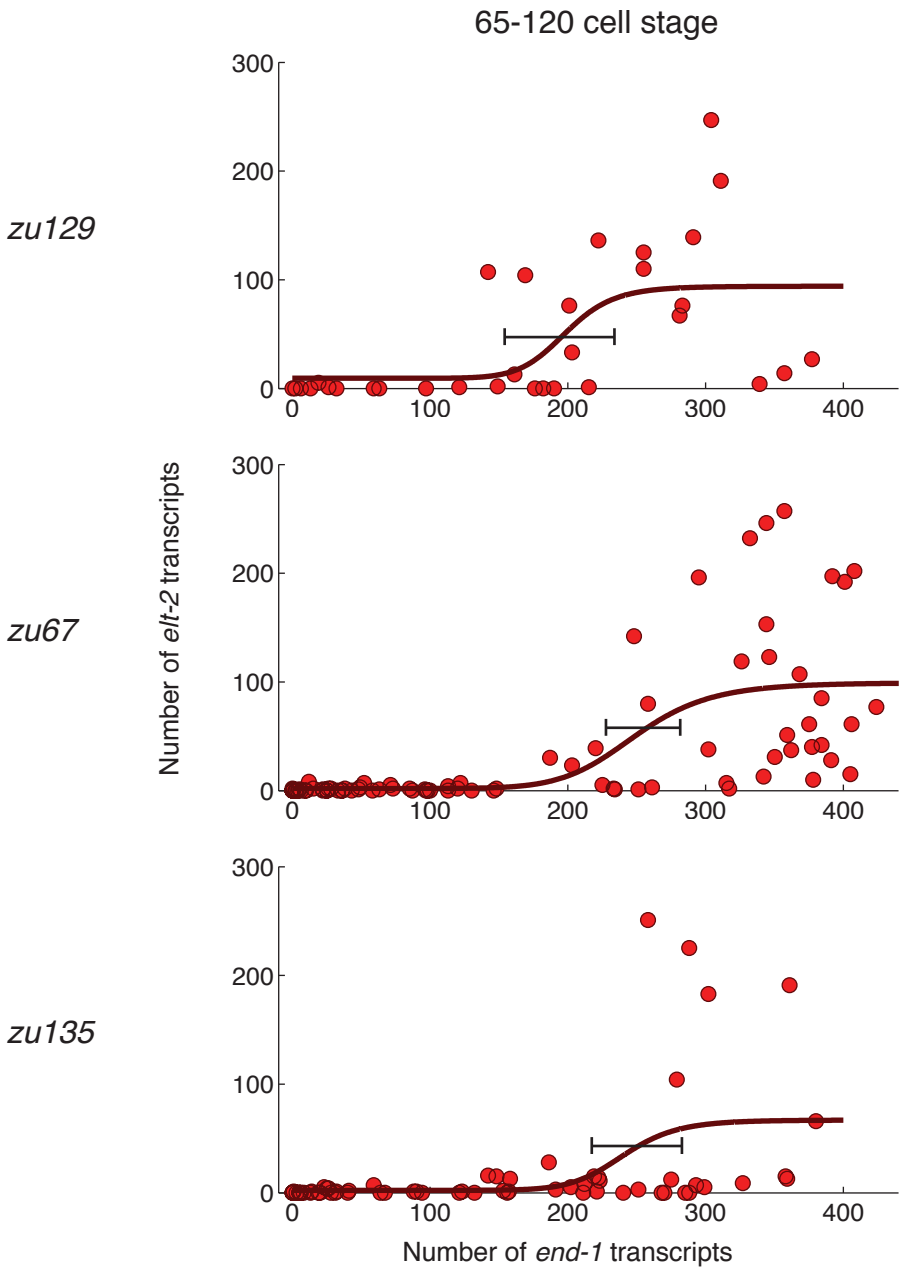

Supplementary Figure 12: Estimation of the threshold number of *end-1* transcripts required for *elt-2* activation in *skn-1* mutant alleles (*zu129*, *zu67*, *zu135*). We fit our data to the Hill equation $y = a + b*x^n/(k^n+x^n)$, where x is the number of *end-1* transcripts, y is the number of *elt-2* transcripts, a and b are the maximum and minimum of the equation and k is the location of the half-maximum. We fit the data by first smoothing and then using a non-linear least squares error minimization; we obtained values for k of 199±40, 253±27 and 250±34 and values of n of 11.5±6.5, 9.0±4.2 and 12.3±5.3 for the *zu129*, *zu67*, *zu135* alleles, respectively. We computed the error on k by fitting bootstrap resampled data. The high values of n indicate a sharp threshold behavior. Note that the values for k are different than the thresholds given in the main text; there, we chose the threshold to be where we started to get values of *elt-2* greater than 50 (our threshold for *elt-2* being considered ON), which will typically be less than k. Our analysis here is mainly intended to statistically quantify the differences in threshold and the threshold-like nature of the dose-response relation between *end-1* and *elt-2*.

Supplementary figure 13

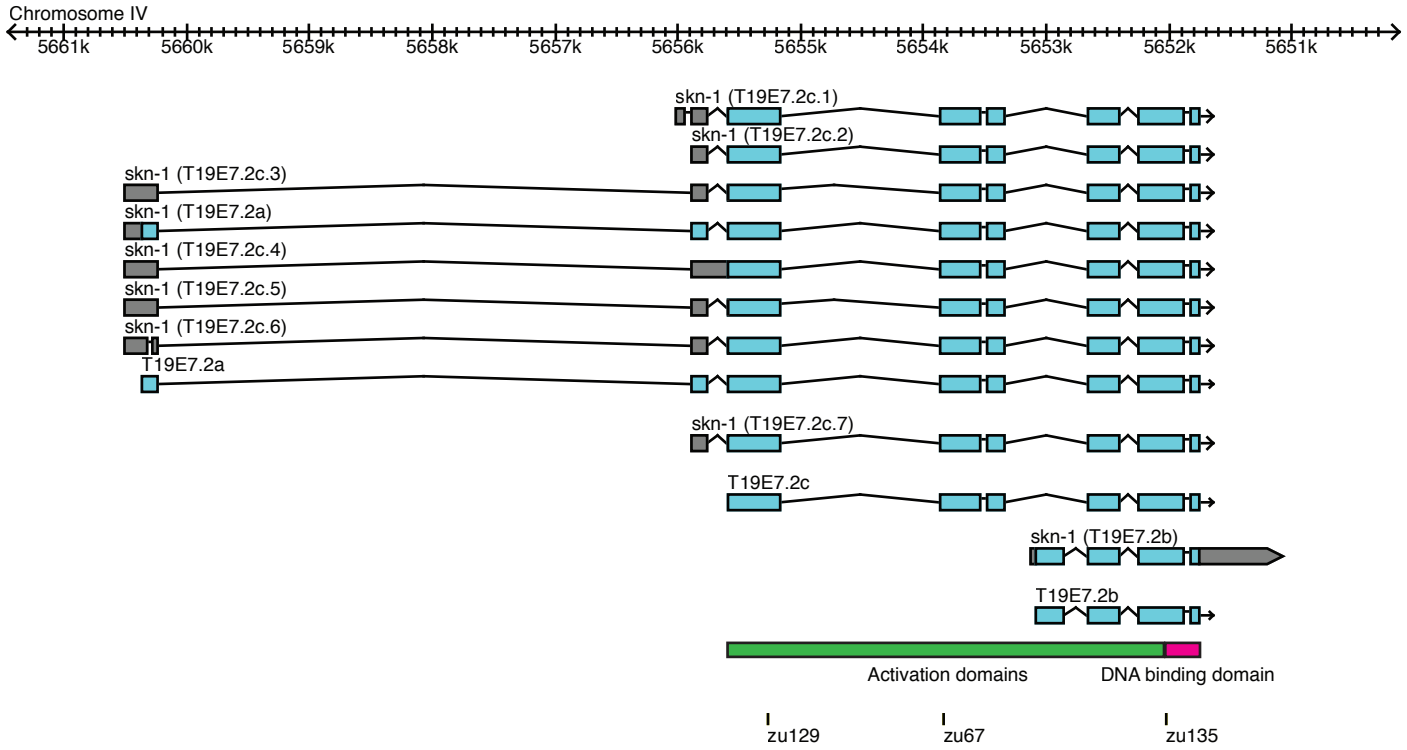

Supplementary Figure 13: Gene model of *skn-1*. *skn-1* encodes many isoforms, all of which contain a DNA binding domain (red) and several activation domains (green; as described in Walker et al., J. Biol Chem, 2000, **275**(29): 22166-71). The mutant alleles described in this paper (*zu129*, *zu67* and *zu135*) are all premature stop codons in the open reading frame of the mRNA, located as indicated. All of the premature stop codons remove the DNA binding domain. Surprisingly, the least penetrant allele (*zu129*) removes the greatest portion of the protein coding sequence of all the mutant alleles. This may indicate a dominant negative effect for the *zu67* and *zu135* alleles. It is also possible the translational readthrough of the premature stop codon leads to some production of full-length SKN-1 protein; the efficiency of this readthrough could be sequence specific. We believe that this is not the case, though, because the number of *skn-1* transcripts is larger in the more penetrant *zu135* strain than in the *zu129* strain (see Supplelementary Figure 14). (Image generated by www.wormbase.org)

Supplementary figure 14

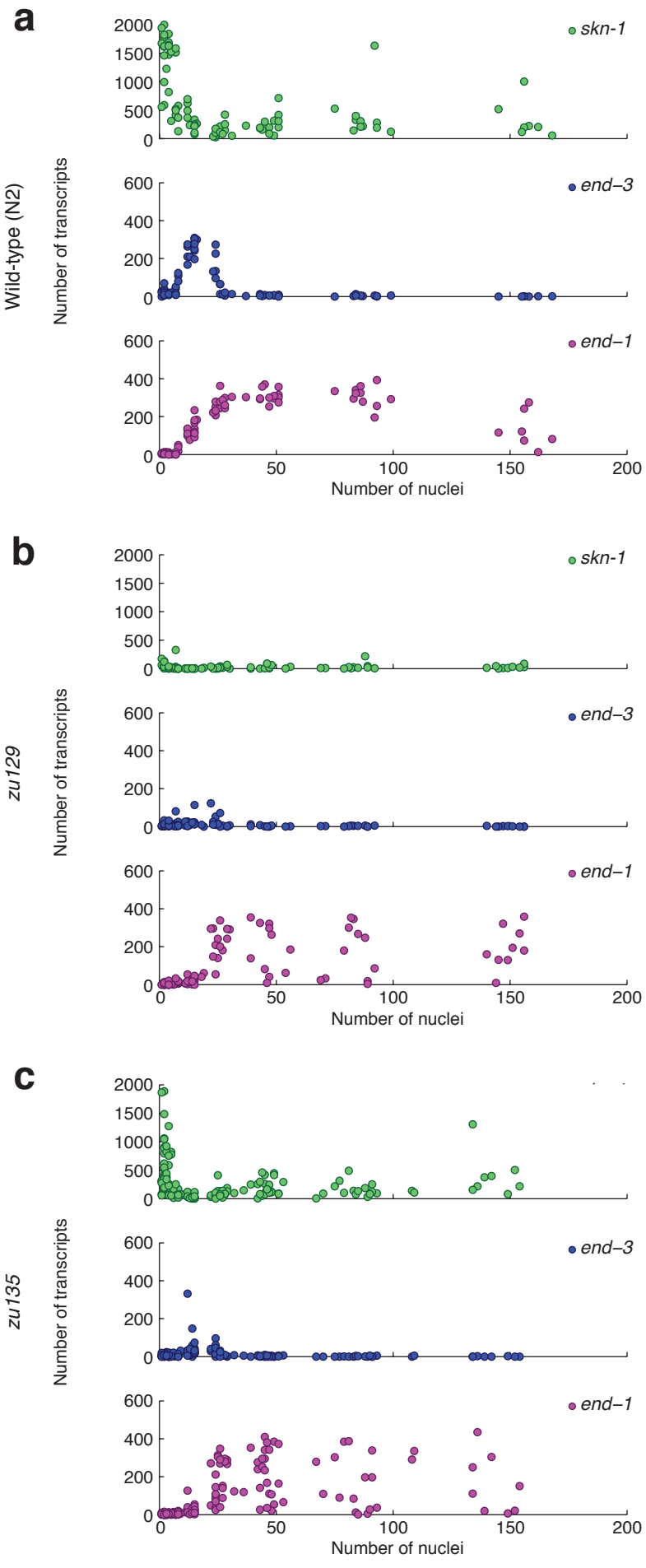

Supplementary Figure 14: Number of *skn-1*, *end-3* and *end-1* transcripts in individual wild-type (N2) and *skn-1* (*zu129* and *zu135*) mutant embryos plotted as a function of the number of nuclei. We labeled the *skn-1* mRNAs with a probes conjugated to the Cy5 dye, while we labeled *end-1* and *end-3* with TMR and Alexa 594, respectively. Owing to poor signal quality for the *skn-1* transcripts, some of the variability in *skn-1* transcript abundance is probably methodological; however, the differences we observed between strains are likely to be real. The purpose of examining differences in *skn-1* transcript abundances was to see if they could account for the differences in penetrance between the different mutant alleles. Our data indicate that this is unlikely, because *skn-1* transcripts are actually more abundant in the more penetrant *zu135* allele. The two *skn-1* mutant alleles possess premature stop codons in different locations within the mutant transcript, and we attribute variation in *skn-1* transcript abundance to differences in the efficiency with which a particular premature stop codon will activate the nonsense-mediate mRNA degradation pathway. It is possible that the large differences in *skn-1* transcript numbers do not correspond with the observed differences in penetrance because the transcripts may be translationally silenced in the somatic lineages.

Supplementary Figure 15

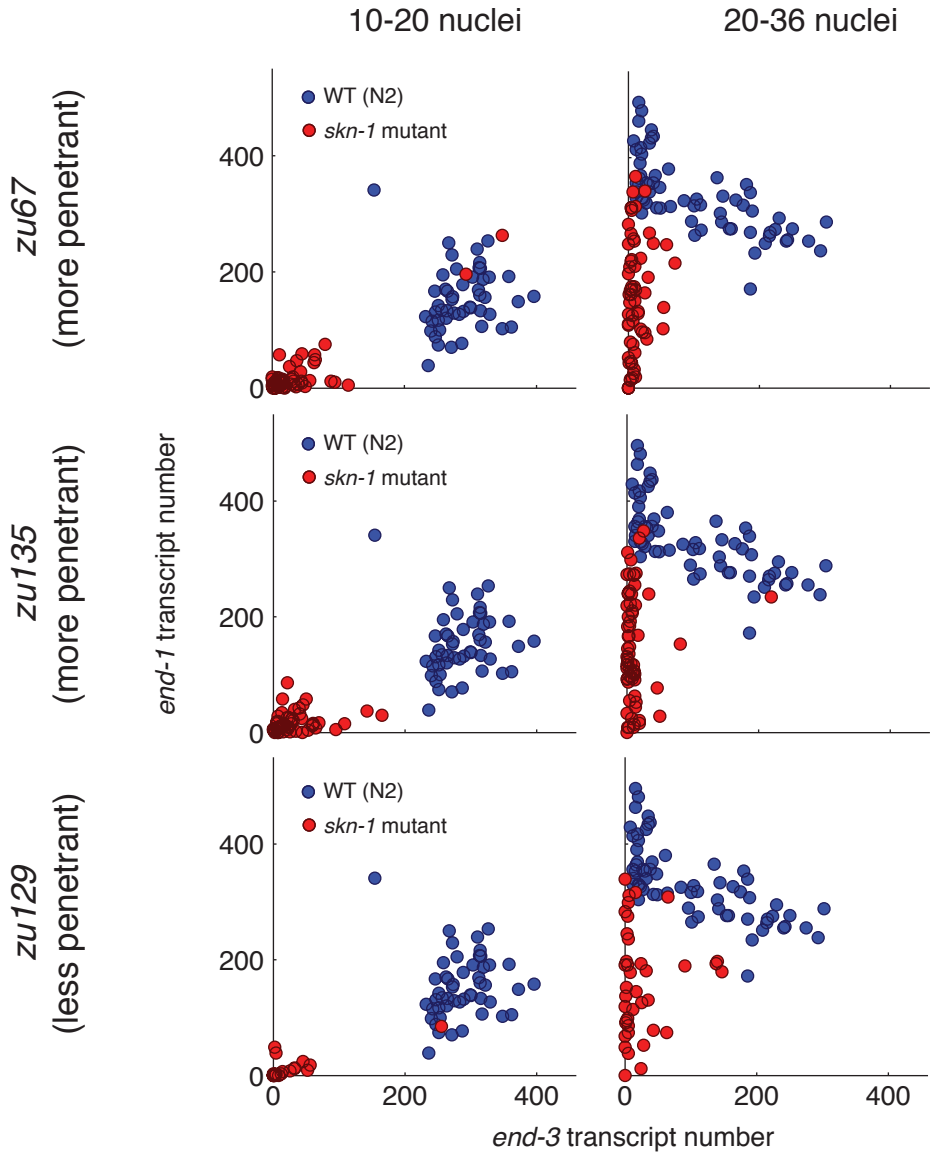

Supplementary Figure 15: Scatter plots of *end-3* and *end-1* transcript numbers in wild-type (N2; blue) and *skn-1* mutant embryos (red) containing between 10 and 20 nuclei (left) or 20 and 36 nuclei (right). We analyzed different mutant alleles of *skn-1* (*zu67*, *zu135* and *zu129*; top, middle, bottom, respectively). We were interested in seeing whether the residual expression of *end-3* was correlated with the variablility in *end-1* expression levels. Between the 10 and 20 cell stages, there is no real correlation beween *end-1* and *end-3* expression, and between the 20 and 36 cell stages, there is a only a mild correlation. These data argue against the possibility that variability in residual levels in *end-3* propagate to variability in *end-1* expression, although it is possible that END-3 protein levels do correlate with *end-1* expression; our methodology is unable to test that possibility, however.

Supplementary figure 16

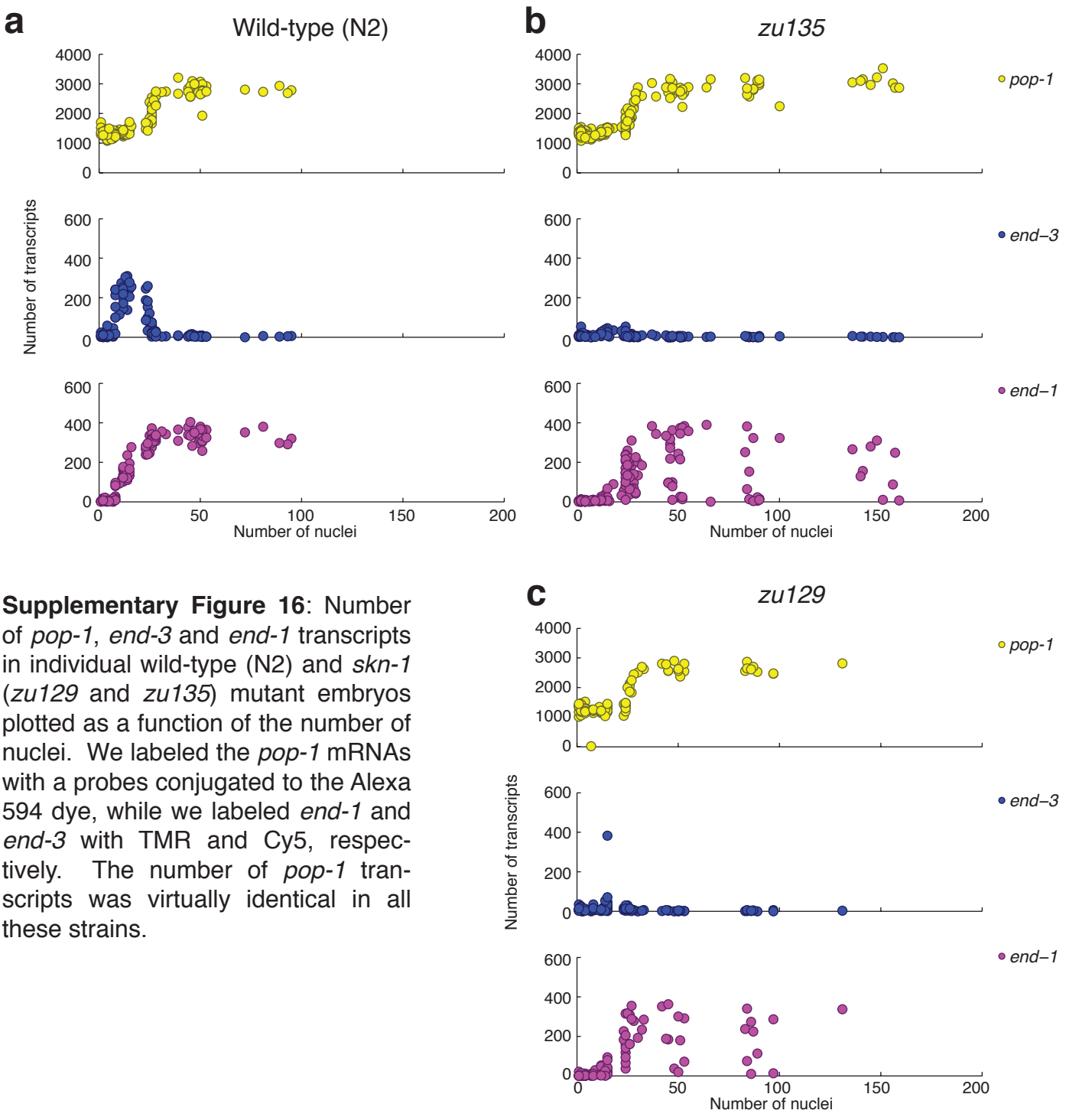

Supplementary Figure 16: Number of *pop-1*, *end-3* and *end-1* transcripts in individual wild-type (N2) and *skn-1* (*zu129* and *zu135*) mutant embryos plotted as a function of the number of nuclei. We labeled the *pop-1* mRNAs with a probes conjugated to the Alexa 594 dye, while we labeled *end-1* and *end-3* with TMR and Cy5, respectively. The number of *pop-1* transcripts was virtually identical in all these strains.

Supplementary figure 17

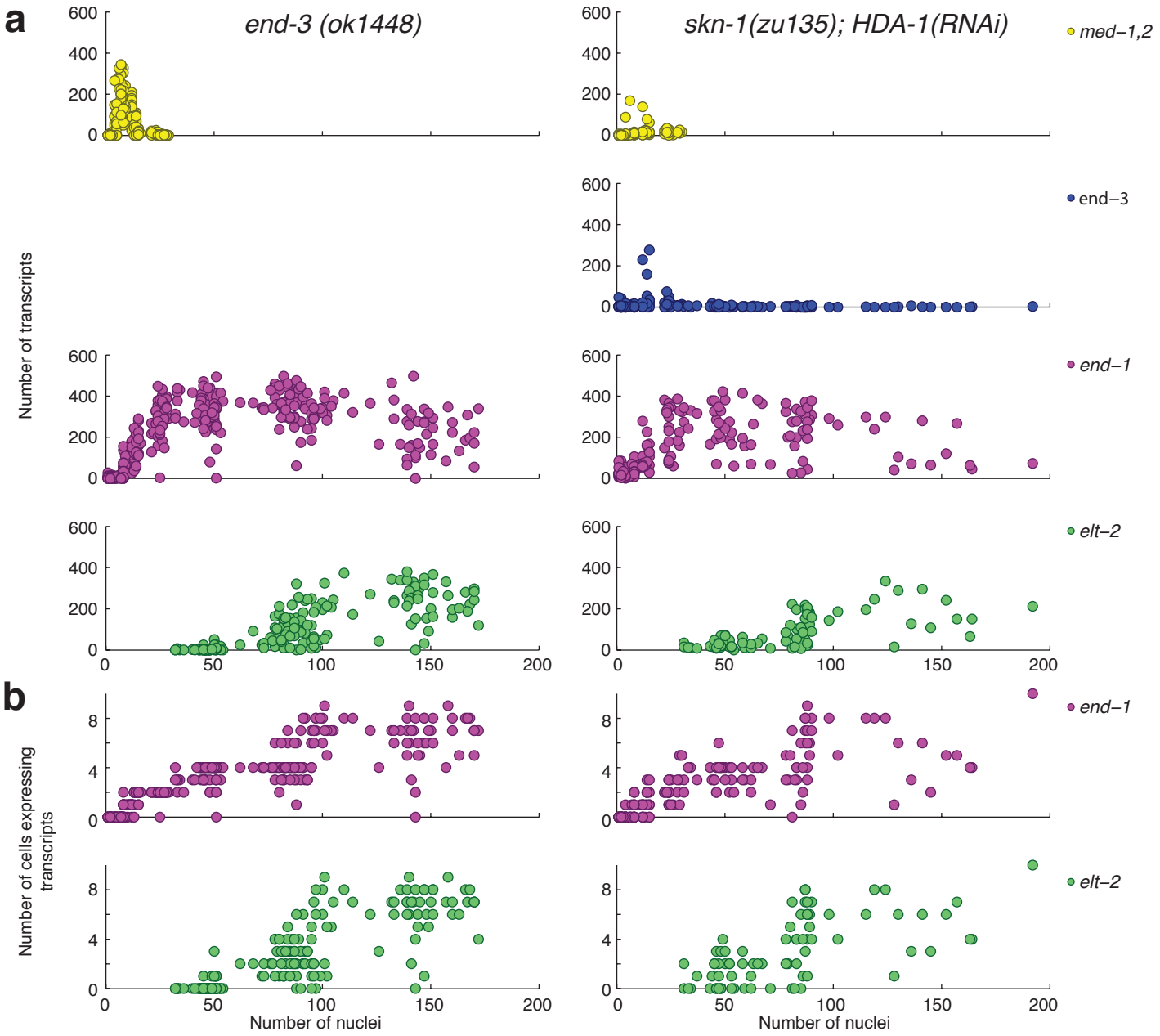

Supplementary Figure 17: **a**. Transcript number vs. number of nuclei for a collection of randomly staged *end-3(ok1448)* and *skn-1(zu135); hda-1(RNAi)* mutant early embryos. **b**. Number of cells expressing *end-1* (top) or *elt-2* (bottom) within individual *end-3(ok1448)* and *skn-1(zu135); hda-1(RNAi)* mutant embryos vs. number of nuclei. Up until the 4E stage, *skn-1(zu135); hda-1(RNAi)* mutant early embryos exhibited some ectopic expression of *end-1*, presumably in the MS cell, as found by Calvo *et al.* EMBO J **20**(24):7197-208 (2008)

Supplementary figure 18

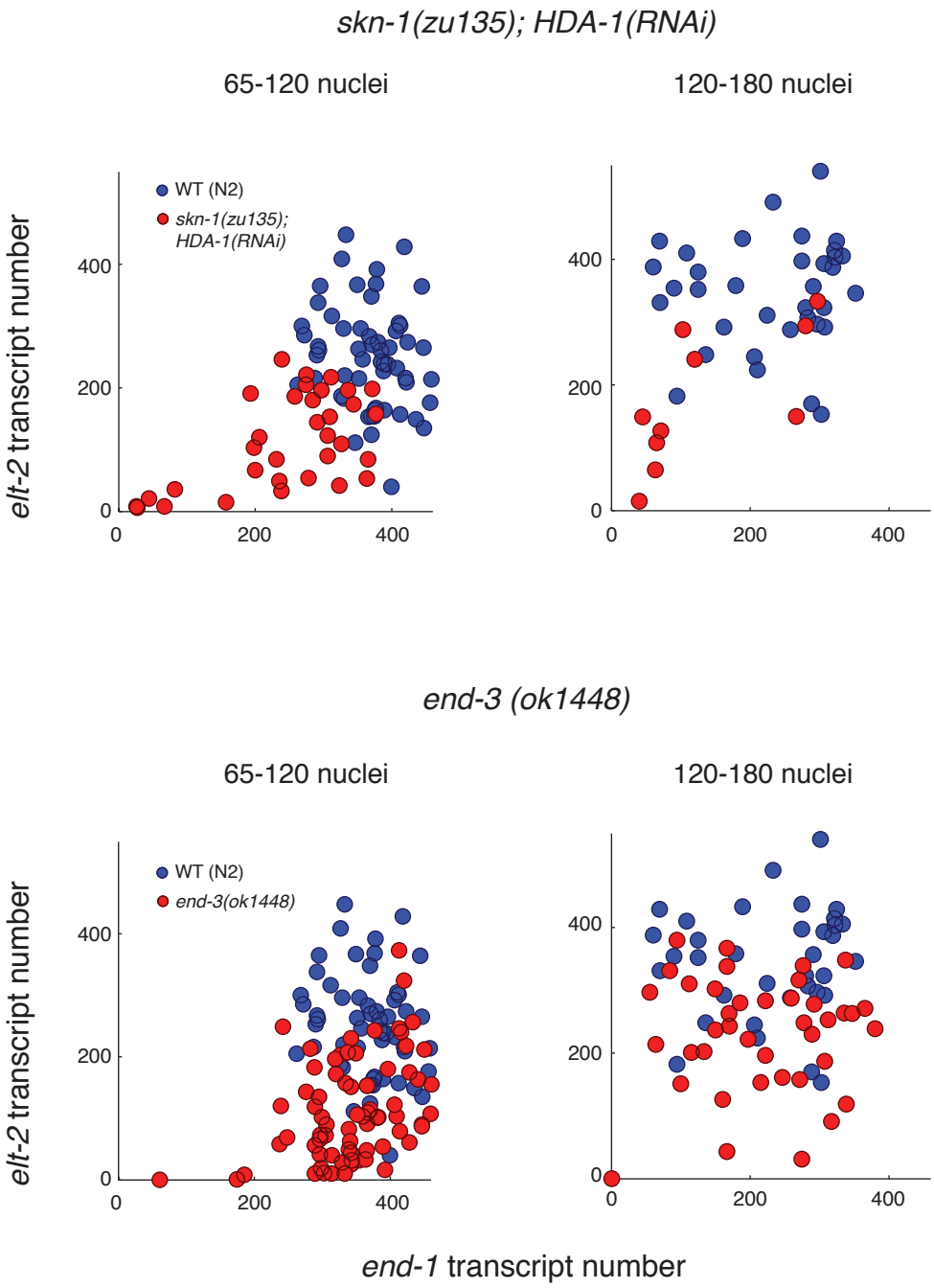

Supplementary Figure 18: Scatter plots of *end-1* vs. *elt-2* transcript numbers in wild-type (N2; blue) and *skn-1(zu135); hda-1(RNAi)* (top) and *end-3(ok1448)* (bottom) mutant embryos (red). Plots on the left represent embryos containing between 65 and 120 nuclei, while plots on the right represent embryos containing between 120 and 180 embryos. The thresholding mechanism still applies to the *skn-1(zu135); hda-1(RNAi)* embryos, which shows that the removal of *hda-1* does not increase *elt-2* expression intrinsically but rather does so by increasing the expression of *end-1*. We also see some indications that a thresholding mechanism applies to in the *end-3(ok1448)* strain (consistent with our data from the *skn-1* mutant strains), although there are relatively few data points at the lower levels of *end-1* expression.

Supplementary figure 19

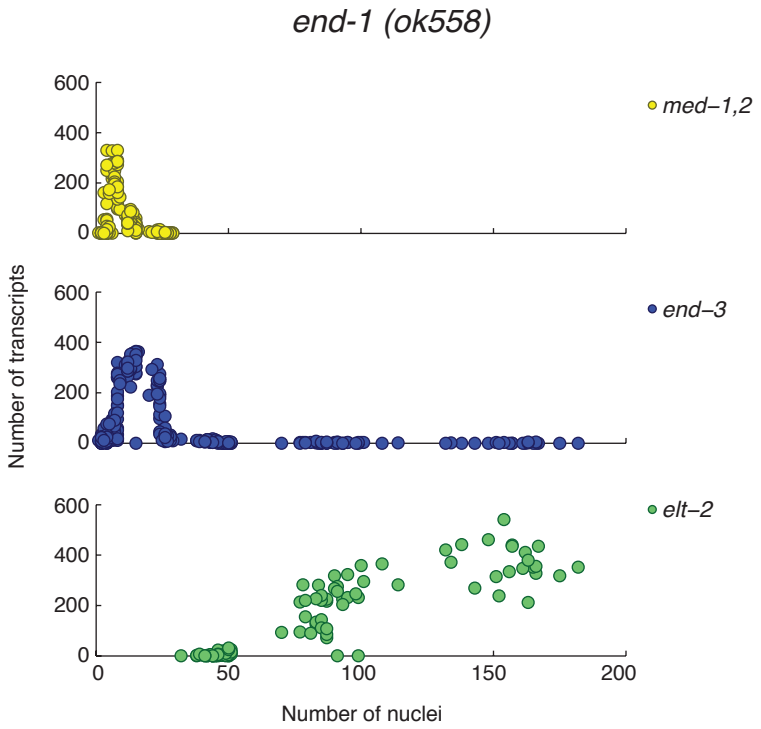

Supplementary Figure 19: Transcript number vs. number of nuclei for a collection of randomly staged *end-1(ok558)* mutant embryos.